Applied Magnetic Resonance (2022) 53:1227–1237
https://doi.org/10.1007/s00723-021-01440-0

Applied
Magnetic Resonance

ORIGINAL PAPER

Solid State Photo-CIDEP in Chiral Linked Systems

I. M. Magin[1,2] · M. Yu. Ivanov[2,3] · N. E. Polyakov[1] · A. I. Kruppa[1] · M. V. Fedin[2,3] · T. V. Leshina[1]

Received: 30 July 2021 / Revised: 1 October 2021 / Accepted: 5 October 2021 /

Abstract

Photoinduced charge transfer processes in diastereomers are currently being intensively studied as models for the binding of chiral drugs to chiral amino acid residues located in the active centers of enzymes and receptors. In this regard, direct detection of paramagnetic forms of diastereomers formed upon UV irradiation is of considerable interest. In the present study, we use photochemically induced dynamic electron polarization (photo-CIDEP) to detect paramagnetic particles resulting from UV irradiation of dyads containing the well-known NSAID (*R*/*S*)-ketoprofen with various electron donors. The use of CIDEP allowed us to detect the triplet state of KP in all studied dyads in the solid state, as well as the product of intramolecular electron transfer in the dyad with tryptophan, namely, the biradical zwitterion (BZ) in solid and liquid states. The difference in the CIDEP spectra of the BZ of RS and SS diastereomers corresponds to the previously predicted based on the analysis of the effects of CIDNP (chemically induced dynamic nuclear polarization).

1 Introduction

Chiral compounds invariably attract the attention of researchers, both in connection with the fundamental problems of the origin of life on the Earth, as well as due to their wide practical application in various fields [1–5]. One of the main fields of their application is pharmacy, since more than half of the drugs have chiral centers [6]. In this regard, linked systems with two chiral centers are widely used as convenient models to study the interaction of chiral drugs with chiral amino acid residues located in active sites of enzymes and receptors [7].

✉ I. M. Magin
magin@kinetisc.nsc.ru

[1] V.V. Voevodsky Institute of Chemical Kinetics and Combustion, 3 Institutskaya Str., Novosibirsk 630090, Russia

[2] Novosibirsk State University, 2 Pirogova Str., Novosibirsk 630090, Russia

[3] International Tomography Center, 3a Institutskaya Str., Novosibirsk 630090, Russia

Studies of model dyads are intended to establish the physical reasons for the differences in the medicinal properties of the enantiomers of chiral drugs. Enantiomers, completely identical in their physicochemical properties, often show differences in medicinal properties, and these differences are a big problem in pharmacology, since drugs are used mainly in racemate form. Another serious problem is the unidentified reasons for the dramatic effect of the appearance of D-tryptophan in their composition instead of L analog on the structure of a number of proteins and peptides. It occurs with aging of living systems, and is currently considered one of the main causes of a number of ailments, including Alzheimer's and Parkinson's diseases [8].

Over the past decade, studies of the processes of photoinduced electron transfer (ET) and hydrogen atom transfer (HT) in donor–acceptor chiral dyads by fluorescence spectroscopy and spin chemistry methods have made it possible to detect stereoselectivity (difference in ET rates of RS and SS optical configurations of diastereomers), as well as spin selectivity (difference in its CIDNP (chemically induced dynamic nuclear polarization) coefficients) [7, 9–12]. Comparison of the experimental differences in the CIDNP coefficients with the calculated ones indicates that they are due to the difference in the hyperfine interaction (HFI) constants in the biradical zwitterion (BZ), from which polarized dyads are obtained as a result of the back ET [12]. In this regard, it becomes clear that further studies of BZ are of considerable interest, especially in terms of the difference between RS and SS optical configurations.

This report is devoted to an attempt to observe biradicals and BZ formed in chiral dyads under UV irradiation using photochemically induced dynamic electron polarization (photo-CIDEP)—direct method of the paramagnetic particles detection. The systems under study are dyads containing an electron acceptor (*R*/*S*)-ketoprofen (KP) and hydrogen and/or electron donors: (*S*)-*N*-methyl pyrrolidine (Pyr), cholesterol (Chl) and (L)-tryptophan (Trp) (Fig. 1). Benzophenone (BP) and KP were also studied as an example of systems that demonstrate triplet CIDEP.

Previous studies by the methods of photochemistry and spin chemistry have shown that under UV irradiation of the solution of dyad 3, 4 and 5 the formation of KP in a triplet excited state occurs. In dyad 4 it is followed by an intramolecular HT, and a parallel ET and HT in dyad 3. Further, the dyads 3 and 4 undergo cyclization in their biradical forms [13, 14]. On the contrary, for diastereomers of the dyad with tryptophan (5) only reversible ET from tryptophan in the singlet excited state to the KP in the ground state takes place [15, 16].

Thus, in the present work, we performed time-resolved EPR measurements (TR-EPR) under the UV irradiation of glass solutions of the aforementioned chiral linked systems. To separate the CIDEP spectra of the triplet state of chromophore from the spectra of biradicals and BZ, the KP (2) and its close analog BP (1) were also investigated. Comparison of the spectra of the triplet CIDEP of KP and BP is also of independent interest, since they noticeably differ in reactivity, and it is believed that the triplet state of KP is more delocalized and has a partial π–π* character [17, 18].

So, final aim of this report is to study the paramagnetic intermediates formed under UV irradiation of dyad 3–5 and to trace the difference between (*R*,*S*) and (*S*,*S*) configurations using the TR EPR technique.

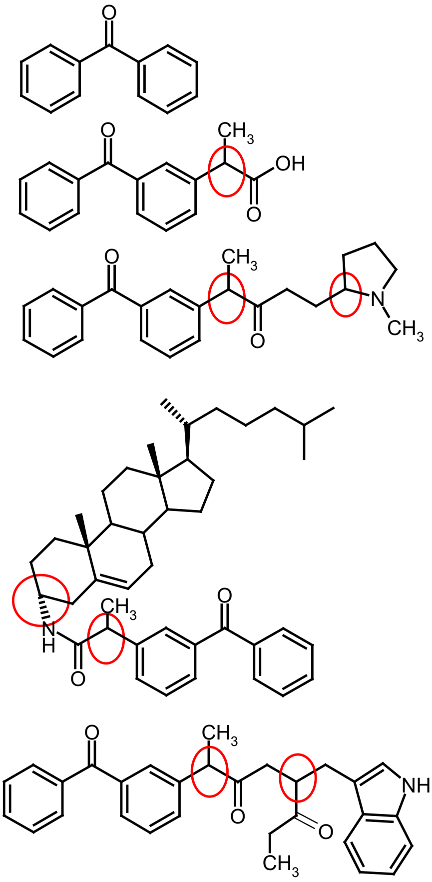

Fig. 1 Structures of ketones KP and BP and chiral dyads. Chiral centers are marked with red ovals. (1) BP, (2) KP, (3) (*R*/*S*) KP-(*S*)Pyr, (4) (*R*/*S*)KP-Chl, (5) (*R*/*S*)KP-(*S*)Trp

2 Experimental Part

Time-resolved EPR measurements were carried out on a home-made (ITC SB RAS) setup based on a commercial continuous wave X-band EPR spectrometer (9 GHz) Bruker EMX. The spectrometer is equipped with a cryostat having optical window, which makes it possible to carry out TR EPR experiments at temperatures of 80–300 K. Most of experiments were carried out in toluene glass solution at 100 K under excitation with a LOTIS-TII Nd: YaG laser at a wavelength of 355 nm with a repetition rate of 10 Hz. Several experiments were carried out at room temperature under the same excitation conditions. The radiation was directly applied to the sample, which was placed in an ER 4118X-MD5 resonator, through the optical window of the cryostat. In the experiment, kinetic dependences were recorded in the nano-microsecond time range in various magnetic fields. As a result, the CIDEP spectra were obtained at different time delays after the laser pulse.

3 Results and Discussion

In all three dyads, under UV irradiation the TR EPR spectra demonstrated the CIDEP effects, presented in the Figs. 2, 3, 4, 5 and 6 and Tables 1 and 2. For convenience in analysis of the obtained effects, the systems are divided into two groups: in one of them, according to the reference data, the main paramagnetic particle should be a biradical, and in the other, a BZ [13–17]. The first group is represented by two dyads: (*R*/*S*)KP-(*S*)Pyr (3) and (*R*/*S*)KP-Chol (4). Two diastereomers of dyad 5: (*R*)KR-(*S*)Trp (5a) and (*S*)KP-(*S*)Trp (5b) under the UV irradiation demonstrate only ET with the formation of BZ.

The CIDEP spectra of dyads 3–4 from the first group, as well as KP (2) and BP (1), at 80–100 K in toluene glass solution are shown in Fig. 2.

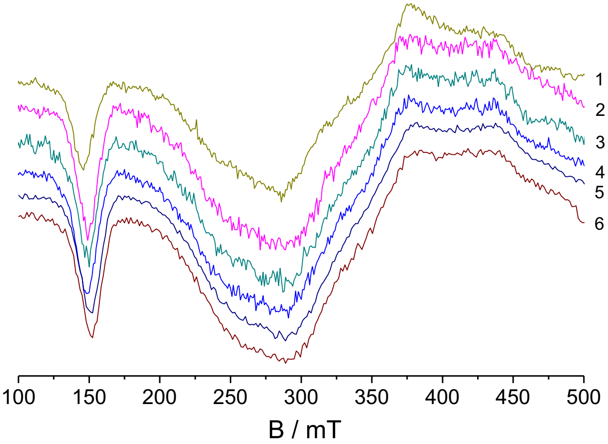

Fig. 2 CIDEP spectra in toluene at 80–100 K. (1) BP, (2) KP, (3) racemate of (*R*/*S*)KP-(*S*)Pyr (the spectrum is shown for comparison, since CIDEP in this dyad was studied earlier [14]), (4) (*S*)KP-(*S*)Pyr, (5) (*S*)KP-Chl, (6) (*R*)KP-Chl. Excitation wavelength $\lambda_{\mathrm{exc}} = 355$ nm

Fig. 3 CIDEP spectra in toluene glass detected at 80–100 K. (1) (*S*)KP-(*S*)Pyr, (2) (*R*)KP-(*S*)Trp, (3) (*S*)KP-(*S*)Trp. Arrows indicate well-defined lines which are absent in spectrum belonging to KP triplet (1). Excitation wavelength is 355 nm

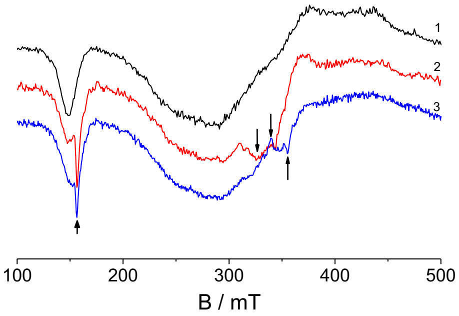

Fig. 4 **a** CIDEP spectra of (S) KP-(S)Trp detected in toluene glass at 100 K, at various delays after laser excitation. Excitation wavelength $\lambda_{exc} = 355$ nm. **b.** CIDEP spectra of (R)KP-(S) Trp in toluene glass at 100 K at various delays after laser excitation. Excitation wavelength $\lambda = 355$ nm.

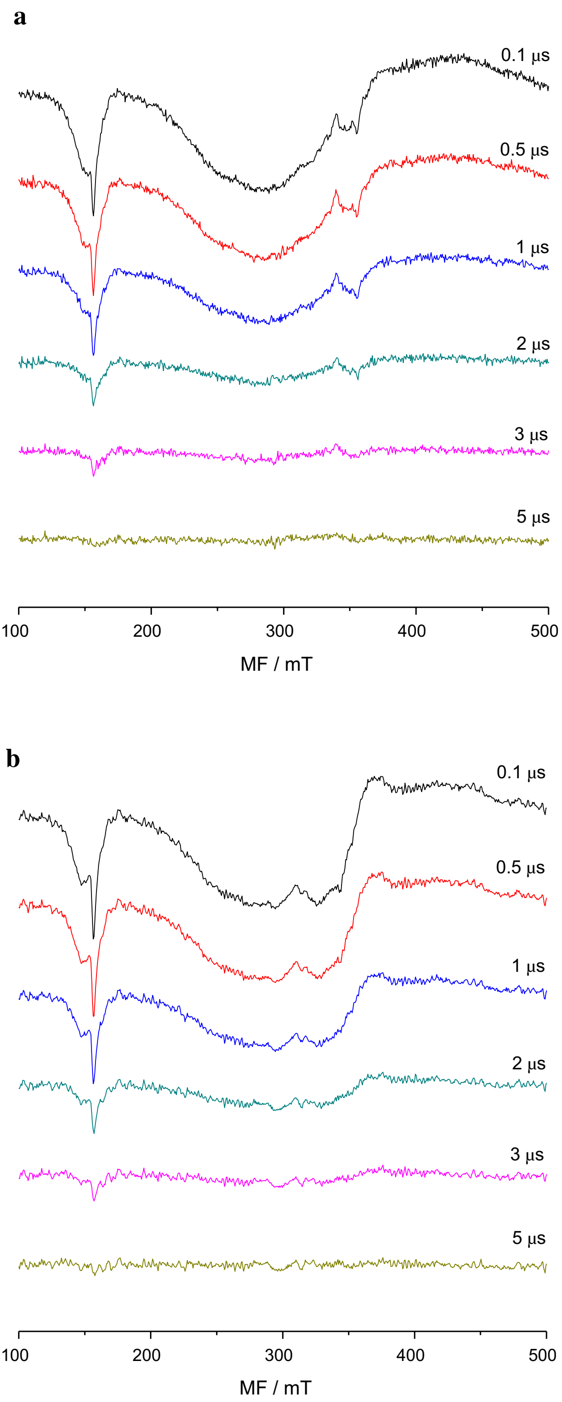

Note that such spectra are characteristic for the triplet mechanism of CIDEP formation in solid state. In this case, CIDEP is formed as a result of difference in the rates of transitions from the excited S state to the T_x, T_y and T_z states. In magnetic field, they are projected onto the states T_0, T_+ and T_-, which are the eigenstates of the system, and the transitions between them are visible in the spectrum. The T_0 state is different in energy from T_+ and T_-, therefore, the transitions T_0–T_+ and T_0–T_- are shifted relative to each other in magnetic field. Due to this separation of the bands in the spectrum, it is possible, for example, to obtain the value of the dipole–dipole interaction of the triplet (D). Since the rotational averaging is suppressed in the glassy state, the spectrum is broadened, and transitions corresponding to different orientations manifest themselves in different fields. Thus, transitions of the *x* and *y* orientations of the molecule appear closer to the center of the spectrum, and the lines located at the ends of the spectrum correspond to the z orientation. Also in the half field, in the region of 150 mT, one can see the double-quantum transition T_+–T_-. Neither the CIDEP spectra, nor the decay times of CIDEP of the dyads 3, 4 and KP show significant differences (Fig. 1; Table 1). This allows us to conclude that the triplet state of the chromophore, KP, makes the dominant contribution to the TR EPR of dyads 3 and 4.

Figure 2 also shows that while the KP spectrum is identical to the spectra of the dyads, the BP spectrum, although close to them, has obvious differences in the shape of the main spectrum, as well as in the position of the peak located in half field. It can be assumed that these differences are due to the difference in electronic structures of KP and BP, which was mentioned above.

Significant zero-field splitting (ZFS), which determines the width of the TR EPR spectrum of the order of 200 mT, are typical for triplet excited molecules [19]. The ZFS values for biradicals with larger distances between electrons are, as a rule, much smaller [20–23].

The identity of the spectra of dyads 3 and 4 and the KP force us to assume that the formation of biradicals does not occur at all in a frozen solution. The basis for this assumption is the fact, that transfer of a hydrogen atom in dyads 3 and 4 which followed by cyclization requires significant rearrangement of molecules. The latter can be difficult in the solid state [13, 14, 17].

Next, the kinetics of the CIDEP signals decay in these systems has been analyzed. The resulting mono-exponential decay times are presented in Table 1.

It can be seen from the Table 1 that all spectral lines of both ketones and dyads 3 and 4 have close decay times in the interval 1.4–2 µs. In the light of the foregoing, namely, the absence of other paths of photodegradation, these times should be attributed to the times of electronic relaxation T_1 of triplet state.

Next, we turn to a discussion of the CIDEP effects in systems from the second group—diastereomers of the (*R*/*S*)KP-(*S*)Trp dyad. This dyad demonstrated reversible intramolecular ET with the formation of BZ, as it was previously shown under photolysis at room temperature [15, 16]. In solutions, this is the ET between Trp in the singlet excited state and KP in the ground state. Since under the conditions of TR EPR experiment light is mainly absorbed by KP, another variant is possible: ET between the excited KP and Trp in the ground state. Previous studies have shown that in this case we can expect the formation of the same BZ [15].

As can be seen from Table 1, there is a noticeable difference between the decay times of 5a, b and 3 and 4 diastereomers. Differences are also seen when we compare the CIDEP spectra of the systems from the first and second groups. Thus, Fig. 3 shows the CIDEP spectra of dyads 5ab, (*R*/*S*)KP-(*S*)Trp, in toluene glass at 100 K in comparison with the spectrum of (*S*)KP-(*S*)Pyr.

Thus, the spectra of the dyads 5ab with tryptophan, in addition to the spectrum of the KP triplet, demonstrate additional peaks that are absent in the dyad 3 with *N*-methylpyrrolidine. The group of additional peaks is in the region of 350 mT. In the half-field, an additional signal is also observed, and it is shifted approximately by 10 mT from the corresponding signal of the KP triplet.

Below are the spectra of diastereomers of the dyad 5 recorded at different time delays (Fig. 4a, b).

Figures 4a, b let one see the different time evolution of the lines of triplet and the additional lines of dyads 5a,b. So, it can be seen that additional lines decay noticeably slower than the triplet spectrum. For example, one can see that the narrow line at 157 mT has a slightly longer decay than the line at 148 mT. These lines are located on the side wing of the triplet line, and if the contribution from base line is removed from its kinetics, then the characteristic decay times can be determined as 1.9 and 1.8 μs for dyads 5a and 5b, respectively (see Table 2).

The decay time dependencies of the lines for dyads 5a,b at 148 and 157 mT are shown in Figs. 5 and 6.

It is worth noting that the decay kinetics of 150 mT, 157 mT lines in the half-field of the RS diastereomer of dyad (5b) also show a longer time and its long-lived components are somewhat more intensive than those detected for the SS-diastereomer (Fig. 4a, b).

Decay times for some other additional lines in the spectra of SS and RS diastereomers of dyad 5 were obtained in a similar way. The decay times of these lines are shown in Table 2.

The line width of additional signals in the spectra of SS and RS dyads in the half field at 157 mT is about 4 mT. The widths of their main spectra for clearly defined components differ significantly and can be estimated about 15 and 30 mT for SS and RS dyads, respectively. Both the lines in the spectrum of the main components and the additional lines in the half-field are substantially narrower than the corresponding components of the triplet spectrum. This spectral width allows us to conclude that the observed spectrum really belongs to the BZ, where, according to the results of quantum chemical calculations of the geometry of the dyads 5a, b, distances between paramagnetic centers in different conformations can vary from 4 to 10 A [15, 16]. If we estimate the dipole–dipole splitting as the width of the spectrum, in point dipole approximation we obtain $r_D = \left(\frac{3}{2}\frac{g_e\beta_e}{D}\right)^{1/3} = 30.3 \cdot D^{-1/3}$ [24], then 15 mT corresponds to the distance between unpaired electrons 5.7 A, and 30 mT to the distance of 4.5 A, which corresponds to the above-mentioned results of geometry calculations of dyads 5a,b. These results were obtained from calculations carried out taking into account a large number of conformations of diastereomers and distances between donor and acceptor fragments [15, 16].

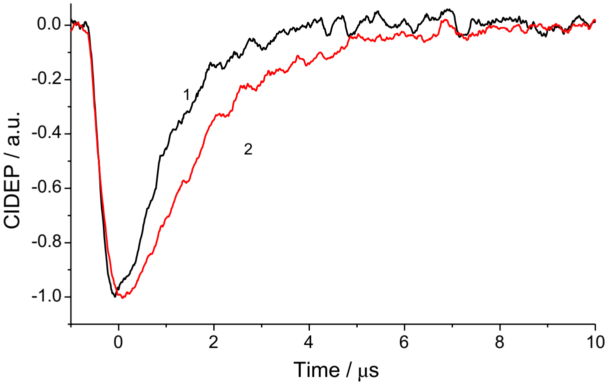

Fig. 5 Time dependences of the CIDEP of (*S*)KP-(*S*)Trp signals in toluene glass at 100 K in a half field. (1) 150 mT, (2) 157 mT. Excitation wavelength 355 nm

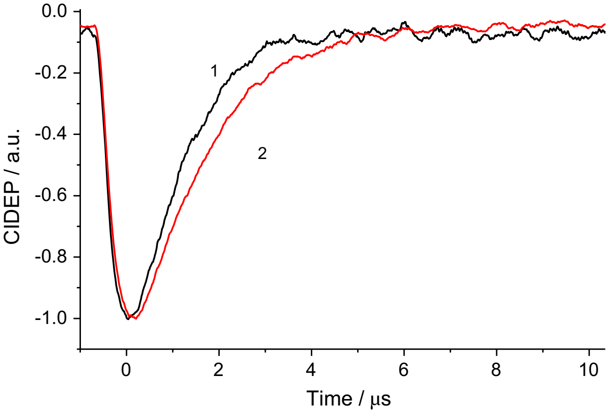

Fig. 6 Time dependences of the CIDEP of (*R*)KP-(*S*)Trp signals in toluene glass at 100 K in a half field. (1) 150 mT, (2) 157 mT. Excitation wavelength 355 nm

Table 1 Times of CIDEP decay for signals at different magnetic fields

τ, μs	149 mT	240 mT	286 mT	376 mT	433 mT
BP (1)	1.7	1.7	1.8	1.9	1.6
KP (2)	1.9	1.9	1.9	2	1.7
(*S*)KP-(*S*)Pyr (3a)	1.9	1.8	2	1.8	1.6
(*R*)KP-(*S*)Pyr (3b)	1.9	1.9	1.9	1.9	1.5
(*S*)KP-Chl (4a)	1.7	1.8	1.8	1.6	1.4
(*R*)KP-Chl (4b)	1.7	1.7	1.7	1.6	1.4
(*S*)KP-(*S*)Trp (5a)	1.0	1.14	1.35	1.0	1.0
(*R*)KP-(*S*)Trp (5b)	1.1	1.15	1.2	1.3	0.9

The error of tau determination does not exceed 0.1 μs

Table 2 Decay times of additional lines in TR EPR spectra of dyad 5 diastereomers

τ, μs	157 mT	340 mT	372 mT
(*S*)KP-(*S*)Trp	1.9	1.8	
(*R*)KP-(*S*)Trp	1.8		1.5

The error of tau determination does not exceed 0.1 μs

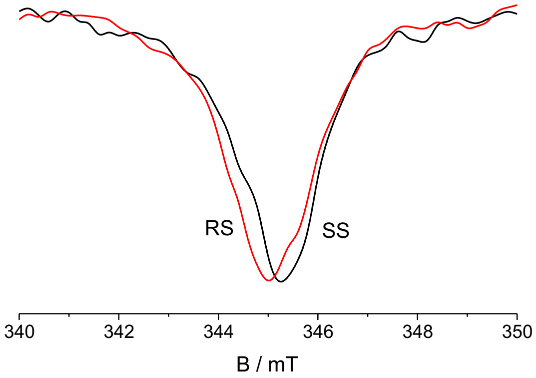

Fig. 7 CIDEP spectra of (*R*)KP-(*S*)Trp and (*S*)KP-(*S*)Trp dyads in toluene at 280 K. Excitation wavelength is 355 nm

The CIDEP signal of dyad 5 was also observed at a temperature of 280 K. The spectra feature are single lines with a width of about 1.9 and 2.0 mT for the RS and SS diastereomers, respectively, with decay times of about 0.45 μs (Fig. 7). Detected difference of BZs g-factors is about 0.0002.

As it was described above, the photolysis of dyad 5 in solutions at room temperature results in formation of BZ. Therefore, the obtained TR EPR spectrum can be confidently attributed to the same BZ.

The absence of CIDEP spectra at room temperature for the other studied dyads is probably due to the chemical transformations of dyads 3 and 4 under UV irradiation. It can be assumed that dyads 3 and 4 could turn into diamagnetic reaction products during the preliminary stages of the experiment, while in dyad 5 such transformations are absent.

4 Conclusion

Thus, studies of TR EPR under UV irradiation of diastereomers of three dyads in toluene glass solution have shown that all systems exhibit CIDEP signals. Comparison of the characteristics of these signals with those for the KP and BP ketones showed that these are the CIDEP signals of the triplet state of KP, which is a part of all three studied dyads. Signals of biradicals, which have to be formed in dyads 3 and 4, were not detected, neither at room temperature nor in glass. At the same time, upon the UV irradiation of dyad 5 diastereomers the BZ formation was detected, both in toluene glass and in the solution at room temperature. In addition the CIDEP spectra for RS and SS configurations of dyad 5 detected at low temperature differ from each other. This result is important, since it is precisely the differences in the conformations of the BZ that were assumed to be the cause of the spin selectivity phenomenon in chiral systems (the difference in the CIDNP effects in diastereomers).

Acknowledgements The authors are grateful to Prof. Miguel A Miranda for kindly providing the cholesterol dyad.

Funding This research was funded by Russian Science Foundation, Grant number 18-13-00047.

Availability of Data and Material Not applicable.

Declarations

Conflict of interest The author declares to have no conficts of interest.

References

1. V.A. Tverdislov, L.V. Yakovenko, A.A. Zhavoronkov, Russ. J. Gen. Chem. (2007). https://doi.org/10.1134/S1070363207110291
2. M. Avalos, R. Babiano, P. Cintas, J.L. Jimenez, J.C. Palacios, L.D. Barron, Chem. Rev. (1998). https://doi.org/10.1021/cr970096o
3. M.C. Jiménez, U. Pischel, M.A. Miranda, J. Photochem. Photobiol. C (2007). https://doi.org/10.1016/j.jphotochemrev.2007.10.001
4. R. Naaman, D. Waldeck, J. Phys. Chem. Lett. (2012). https://doi.org/10.1021/jz300793y
5. P. Levkin, A. Kokorin, V. Schurig, R. Kostyanovsky, Chirality (2006). https://doi.org/10.1002/chir.20242
6. G.Q. Lin, Q.D. You, J.F. Cheng, *Chiral Drugs: Chemistry and Biological Action* (Wiley, Hoboken, 2011)
7. A.A. Ageeva, E.A. Khramtsova, V.F. Plyusnin, M.A. Miranda, T.V. Leshina, Naproxen, in *Chemistry. Clinical Aspects and Effects*. ed. by J. Horner (Nova, New York, 2018), p. 35
8. J.A. Raskatov, D.B. Teplow, Sci Rep. (2017). https://doi.org/10.1038/s41598-017-10525-5
9. A.A. Ageeva, E.A. Khramtsova, I.M. Magin, N.E. Polyakov, M.A. Miranda, T.V. Leshina, in *Chirality from Molecular Electronic States*, vol. 5, ed. by T. Akitsu (IntechOpen, London, 2019), vol. 5, p. 1. https://doi.org/10.5772/intechopen.82684
10. E.A. Khramtsova, D.V. Sosnovsky, A.A. Ageeva, E. Nuin, M.L. Marin, P.A. Purtov, S.S. Borisevich, S.L. Khursan, H.D. Roth, M.A. Miranda, V.F. Plyusnin, T.V. Leshina, Phys. Chem. Chem. Phys. (2016). https://doi.org/10.1039/C5CP07305G
11. E.A. Khramtsova, A.A. Ageeva, A.A. Stepanov, V.F. Plyusnin, N.V. Leshina, Z. Phys. Chem. (2017). https://doi.org/10.1515/zpch-2016-0842
12. A.A. Ageeva, E.A. Khramtsova, I.M. Magin, D.A. Rychkov, P.A. Purtov, M.A. Miranda, T.V. Leshina, Chem. A Eur. J. (2018). https://doi.org/10.1002/chem.201705863
13. D. Neshchadin, F. Palumbo, M.S. Sinicropi, I. Andreu, G. Gescheidt, M.A. Miranda, Chem. Sci. (2013). https://doi.org/10.1039/C3SC22109A
14. N. Polyakov, A. Ageeva, A. Kiryutin, V. Timoshnikov, I. Magin, S. Babenko, P. Kuznetsova, A. Kruppa, P. Purtov, A. Stepanov, M. Ivanov, M. Fedin, L. Kuibida, T. Leshina, J. Chem. Phys. (2019). https://doi.org/10.1063/1.5128043
15. A.A. Ageeva, S.V. Babenko, I.M. Magin, V.F. Plyusnin, P.S. Kuznetsova, A.A. Stepanov, S.F. Vasilevsky, N.E. Polyakov, A.B. Doktorov, T.V. Leshina, Int. J. Mol. Sci. (2020). https://doi.org/10.3390/ijms21155370

16. A.A. Ageeva, I.M. Magin, A.B. Doktorov, V.F. Plyusnin, P.S. Kuznetsova, A.A. Stepanov, A.A. Alekseev, N.E. Polyakov, T.V. Leshina, Int. J. Mol. Sci. (2021). https://doi.org/10.3390/ijms22126198
17. S. Abad, F. Boscá, L. Domingo, S. Gil, U. Pischel, M.A. Miranda, J. Am. Chem. Soc. (2007). https://doi.org/10.1021/ja0712827
18. S.V. Babenko, P.S. Kuznetsova, N.E. Polyakov, A.I. Kruppa, T.V. Leshina. (2020). https://doi.org/10.1016/j.jphotochem.2020.112383
19. M.Y. Ivanov, S.L. Veber, S.A. Prikhod'ko, N.Y. Adonin, E.G. Bagryanskaya, M.V. Fedin, J. Phys. Chem. B. (2015). https://doi.org/10.1021/acs.jpcb.5b06792
20. S.E. Tolstikov, E.V. Tretyakov, D.G. Mazhukin, I.F. Zhurko, M.V. Fedin, G.V. Romanenko, A.S. Bogomyakov, D.E. Gorbunov, N.P. Gritsan, V.I. Ovcharenko, O.N. Chupakhin, Chem. Eur. J. (2016). https://doi.org/10.1002/chem.201602049
21. S. Tolstikov, E. Tretyakov, S. Fokin, E. Suturina, G. Romanenko, A. Bogomyakov, D. Stass, A. Maryasov, M. Fedin, N. Gritsan, V. Ovcharenko, Chem. Eur. J. (2014). https://doi.org/10.1002/chem.201302681
22. A.V. Bogdanov, B.Y. Mladenova Kattnig, A.Kh. Vorobiev, G. Grampp, A.I. Kokorin, J. Phys. Chem. B. (2020). https://doi.org/10.1021/acs.jpcb.0c08457
23. A.V. Bogdanov, R. Tamura, A.Kh. Vorobiev, Chem. Phys. Lett. (2020). https://doi.org/10.1016/j.cplett.2020.137432
24. V.N. Parmon, A.I. Kokorin, G.M. Zhidomirov, *Stable Biradicals* (Nauka, Moscow, 1980), p. 125